

# Interocular Symmetry of Abnormal Multifocal Electroretinograms in Adolescents with Diabetes and No Retinopathy

Michal Laron,<sup>1</sup> Marcus A. Bearse, Jr,<sup>1</sup> Kevin Bronson-Castain,<sup>1</sup> Soffia Jonasdottir,<sup>2</sup> Barbara King-Hooper,<sup>2</sup> Shirin Barez,<sup>1</sup> Marilyn E. Schneck,<sup>1</sup> and Anthony J. Adams<sup>1</sup>

**PURPOSE.** To investigate, in adolescents with type 1 diabetes and no retinopathy, the spatial correspondence between abnormal multifocal electroretinogram (mfERG) responses in the two eyes.

**METHODS.** mfERG and fundus photographs were measured in both eyes of 68 adolescents with type 1 diabetes and no retinopathy (13 to 19 years old; best corrected visual acuity  $\geq$  20/20), and 30 age-matched controls. The mfERG stimulus was comprised of 103 hexagons, and subtended 45°. mfERG implicit times (IT) and amplitudes (AMP) were derived. Fifteen patients for IT, and five for AMP with at least one eye defined as abnormal (six or more locations with abnormal Z-scores;  $P < 0.03$ ) were analyzed.

**RESULTS.** Nasal retina had significantly more abnormal IT locations compared with temporal retina ( $P = 0.015$ ), and the opposite was true with regard to abnormal AMP ( $P < 0.001$ ). The proportion of abnormal responses in the superior retina was not significantly different from that in the inferior retina ( $P > 0.1$  for IT and AMP). Interocular correspondence of locations with abnormal mfERG IT was significant for all 15 patients ( $P$  values  $< 0.0001$ – $0.012$ ), and agreement between eyes was 68% to 94% (AC1 agreement coefficient: 0.48–0.94). Overall interocular correspondence was also significant ( $P < 0.0002$ ), with 86% agreement (AC1 = 0.76). Overall interocular correspondence of locations with abnormal mfERG AMP was also significant ( $P < 0.0002$ ).

**CONCLUSIONS.** Interocular spatial correspondence of abnormal mfERG responses exists in adolescents with type 1 diabetes and no retinopathy. This is most apparent for IT abnormalities. This correspondence could be used in clinical trials, and raises the possibility of initiating treatment in both eyes at early disease stages as new topical treatments emerge. (*Invest Ophthalmol Vis Sci.* 2012;53:316–321) DOI:10.1167/iovs.11-8825

**T**ype 1 (insulin dependent) diabetes can be diagnosed at any age, but is usually diagnosed in children and young adults. Due to the relatively early onset and long duration of the disease, patients are at risk to develop long-term neurologic,

macrovascular, and microvascular complications. Diabetic retinopathy is one of the major complications in diabetes, affecting approximately half of patients with disease duration greater than 10 to 15 years, and can lead to vision loss and blindness.<sup>1,2</sup> In addition to patients' disability, care and treatment when vision loss already exists puts tremendous economic burden on the federal government.<sup>3,4</sup>

Maintaining good glycemic control remains the gold standard of diabetes treatment. However, recent identification of genetic markers, and better understanding of the mechanisms leading to diabetic retinopathy, may lead to the development of new, early treatments. Early intervention was shown to change the course of the disease and reduce the risk of vision loss.<sup>5</sup> Diagnosis of retinal abnormalities at an early stage, even before clinical evidence of retinopathy exists, can be beneficial, first in treating the disease effectively, and second in reducing the costs of treatment.<sup>5,6</sup>

Our laboratory has previously shown that, in adult patients with diabetes, delays in the implicit times (IT) of the multifocal electroretinogram (mfERG), an electrodiagnostic test of the function of retinal cells, have predictive value for the development of diabetic retinopathy.<sup>7–11</sup> Recently, we have shown that many adolescents with diabetes show delays of the mfERG in the absence of clinical signs of diabetic retinopathy.<sup>12,13</sup>

Intraindividual symmetries in abnormalities between right and left eyes were previously seen in patients with bilateral drusen and age-related macular degeneration despite wide interindividual phenotypic expression.<sup>14,15</sup> More relevant is the symmetry found in the severity of hemorrhages, exudates, and neovascularization between corresponding retinal quadrants in eyes of patients with diabetic retinopathy.<sup>2</sup>

Correspondence in the locations of functional retinal abnormalities between the right and left eyes could be of practical use in two ways. First, clinical trials could use this information to test the efficacy of newly developed topical treatments. The effect of a drug could be assessed when treatment is given in only one eye and a comparison of retinopathy (or functional abnormality) progression is performed between eyes. Second, if correspondence in the locations of abnormalities between right and left eyes exists, local treatment could be applied to both eyes at early stages even if one eye shows more abnormality than the other.

In this study, we investigated whether symmetry in the locations of abnormal mfERG responses exists between the right and left eyes of adolescents with type 1 diabetes before clinical signs of retinopathy are present. We found strong symmetry between eyes for the locations of abnormal mfERG delays, and a weaker symmetry between eyes for locations of abnormal mfERG amplitudes in the adolescent patients.

From the <sup>1</sup>School of Optometry, University of California, Berkeley, California; and <sup>2</sup>Children's Hospital and Research Center Oakland, Oakland, California.

Supported by the Juvenile Diabetes Research Foundation International (JDRF) 8-2008-823 (MAB) and NEI EY02271 (AJA).

Submitted for publication October 19, 2011; revised December 1, 2011; accepted December 2, 2011.

Disclosure: **M. Laron**, None; **M.A. Bearse, Jr**, None; **K. Bronson-Castain**, None; **S. Jonasdottir**, None; **B. King-Hooper**, None; **S. Barez**, None; **M.E. Schneck**, None; **A.J. Adams**, None

Corresponding author: Michal Laron, 360 Minor Hall, Berkeley, CA 94720; mlaron@berkeley.edu.

TABLE 1. Demographics of the Patients and Control Subjects Included in the Analysis

	Age Range (y), (Mean $\pm$ SD)	Sex (Male/Female)	BCVA	Diabetes Duration (y), Mean $\pm$ SD	Hba1c (%), Mean $\pm$ SD
Diabetes IT Analysis ( $n = 15$ )	13–19 (15.5 $\pm$ 1.9)	4/11	20/20 or better	7.2 $\pm$ 4.5	10.2 $\pm$ 2.3
Diabetes AMP Analysis ( $n = 5$ )	14–19 (16.4 $\pm$ 2.4)	2/3	20/20 or better	5.2 $\pm$ 1.4	10.5 $\pm$ 1.8
All Diabetes ( $n = 19$ )	13–19 (15.5 $\pm$ 1.5)	6/13	20/20 or better	6.7 $\pm$ 4.2	10.1 $\pm$ 2.1
Controls ( $n = 30$ )	13–21 (18 $\pm$ 2.8)	11/19	20/20 or better	N/A	N/A

One patient had abnormal IT as well as AMP. N/A, not applicable.

## METHODS

### Subjects

Seventy-eight adolescents diagnosed with type 1 diabetes and 30 healthy controls were screened for this study. Patients were recruited from the Children's Hospital and Research Center Oakland, in Oakland, CA (CHRCO), Department of Endocrinology.

Digital fundus photos (50°) were taken through a dilated pupil from all subjects at the time of testing. These were graded by a retina specialist who was masked to the individuals' identity, to exclude the presence of diabetic retinopathy. Subjects with retinopathy ( $n = 11$ ) were excluded from the study (both eyes from each subject were required to be free of retinopathy for symmetry analysis). Other exclusion criteria were refractive error with spherical equivalent  $< -6.00$  or  $> +4.00$  diopters (D), and diseases other than diabetes that could affect the visual system.

Out of 67 patients with no retinopathy, 48 had fewer than six abnormal IT or amplitudes (AMP) locations in either eye and were not analyzed. Nineteen patients were qualified to be included either in the interocular symmetry analysis of mfERG IT ( $n = 15$ ), or in the analysis of AMP ( $n = 5$ ), and one patient was included in both the IT and AMP analyses, as described later in Methods.

The ages of the patients and controls included in the analyses ranged between 13 and 21 years with mean  $\pm$  SD of 15.5  $\pm$  1.5 years old for patients (male [M]/female [F] = 6/13), and 18.0  $\pm$  2.8 for control subjects (M/F = 11/19). Best-corrected visual acuity (BCVA) of all subjects was 20/20 or better. Mean duration of diabetes was 6.7  $\pm$  4.2 years (Table 1). Patients' glycosylated hemoglobin (HbA1c; an estimate of the average blood glucose over the past 1 to 3 months), measured at the time of visit (DCA2000; Bayer HealthCare, Elkhart, IN), ranged from 6.7% to over 14.0% (mean  $\pm$  SD, 10.1  $\pm$  2.1).

All procedures were explained before testing and informed consent was obtained from all subjects and parents/legal guardians of minors.

Procedures adhered to the tenets of the Declaration of Helsinki, and the University of California Committee for Protection of Human Subjects approved this research.

### Multifocal Electroretinogram

Multifocal electroretinograms (mfERGs) were recorded using a multifocal system (VERIS Science 4.3; EDI, San Mateo, CA). The stimulus was comprised of 103 hexagons scaled in size for cone density, and subtended approximately 45° diameter (Fig. 1A). Each of the hexagons followed a pseudorandom sequence (m-sequence) that modulated it between black ( $<3$  cd/m<sup>2</sup>) and white (200 cd/m<sup>2</sup>). A cathode ray tube (CRT) monitor with a refresh rate of 75 Hz was used for recording. The monitor was a part of a system with a refractor unit, and an infrared eye camera that allowed the examiner to monitor the subjects' eye position and movements. Pupils were dilated fully with 1.0% tropicamide and 2.5% phenylephrine, and the cornea was anesthetized with 0.5% proparacaine. Monocular retinal responses were acquired using a bipolar contact lens electrode (Hansen Ophthalmic, Solon City, IA), and a ground electrode was clipped to the right earlobe. For all subjects the right eye was tested first while the left eye was occluded. There was a 15-minute break to allow for light adaptation before recording from the left eye.

The first order mfERG kernel was analyzed to measure response AMP, calculated as the difference in voltage between the N1 trough and P1 peak, and IT calculated as the time between the local flash and the P1 peak (Fig. 1B). The Hood and Li<sup>16</sup> template scaling technique was used to measure each of the 103 local responses. In brief, the technique uses a template (an average response waveform from control subjects) at each of the 103 locations to fit to the responses. The template is fitted to the response waveforms by varying three parameters. The first parameter shifts the template vertically to account for differences in baseline. The second parameter scales the template amplitude, and the third parameter scales the time vector. A more

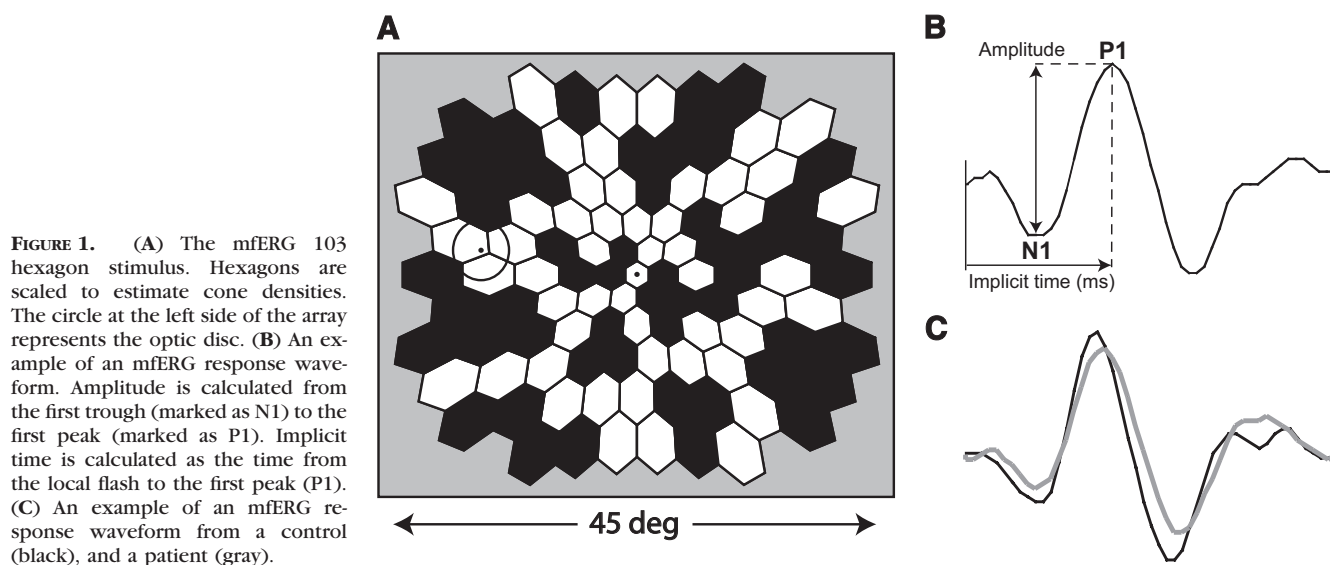


FIGURE 1. (A) The mfERG 103 hexagon stimulus. Hexagons are scaled to estimate cone densities. The circle at the left side of the array represents the optic disc. (B) An example of an mfERG response waveform. Amplitude is calculated from the first trough (marked as N1) to the first peak (marked as P1). Implicit time is calculated as the time from the local flash to the first peak (P1). (C) An example of an mfERG response waveform from a control (black), and a patient (gray).

detailed description of the mfERG procedure can be found in previous reports.<sup>7,17-19</sup> Figure 1C shows an example of an mfERG response from a control subject (black trace), and a patient (gray trace).

### Data Analysis

At each of 103 retinal locations, the mean and SD from the control subjects were used to generate a Z-score value for each response. Retinal locations with Z-scores  $\geq 2$  for IT and  $\leq -2$  for AMP were considered as abnormal ( $P < 0.023$  for both). An eye with 6 or more abnormal locations was defined as abnormal ( $P < 0.03$ ). Interoocular symmetries of the abnormal retinal locations were analyzed only in patients with at least one eye defined as abnormal. The reasoning behind this was to have enough abnormal retinal locations for a valid statistical analysis (e.g., if both eyes were completely normal, there would be perfect but uninteresting symmetry). The demographics of the 15 patients who qualified for IT and the 5 who qualified for AMP symmetry analysis were a good representation of the entire group of patients.

### Statistical Analysis

Potential difference between upper and lower retina in terms of frequency of abnormality was tested by evaluating whether the proportion between the number of abnormal hexagons and the total number of hexagons at the lower retinas was significantly different from the proportion in upper retinas. Difference between nasal versus temporal retina was evaluated similarly.

Fisher's exact probability test was used to examine whether symmetry exists between locations with abnormal mfERG in right versus left eye. Fisher exact is similar to  $\chi^2$  statistic and is more accurate in cases where at least one of the cells in a  $2 \times 2$  table has  $< 5$  observations. It is important to note that, at any mfERG location, both eyes may present agreement in classification (normal or abnormal) just by chance. To estimate the symmetry in locations defined by the mfERG as abnormal with a correction for chance agreement, we used the AC1 agreement coefficient statistic rather than the commonly used Kappa statistic. The Kappa statistic is highly sensitive to the prevalence of a trait (how normal or abnormal an eye is). In cases in which both eyes of an individual are either relatively healthy or sick (high agreement that both eyes are normal or abnormal), the AC1 coefficient statistic is less affected by the prevalence of a trait and will more accurately represent the true agreement.<sup>20-22</sup> An AC1 value of zero represents no agreement beyond chance, while a value of 1 represents perfect agreement.

### RESULTS

Of the 67 patients, 15 (22%) had at least one eye defined as abnormal by mfERG IT, and 5 (7%) had at least one eye defined

as abnormal by mfERG AMP. Only one patient (1.5%) had local abnormalities in both IT and AMP.

Across the 15 patients (both eyes from each patient) with abnormal IT, the nasal retina had significantly more locations with abnormal IT compared to the temporal retina ( $P = 0.015$ ; Fig. 2, left). The distribution of AMP abnormalities showed the opposite trend in the five patients with abnormal AMP ( $P = 0.0007$ ; Fig. 2, right illustration). However, it is important to note that this trend is based on a small sample size (five patients). In contrast, the proportion of hexagons defined as abnormal in the superior retina was not significantly different from the proportion in the inferior retina ( $P = 0.90$  for IT, and  $P > 0.99$  for AMP).

Figure 3 shows examples of the locations of abnormal IT regions in the right and left eyes for two of the patients. In the example, both patients show significant symmetries between eyes, with many corresponding abnormal mfERG IT locations ( $P < 0.0001$  for both patients). Symmetries were significant for all 15 patients with  $P$  values ranging from  $< 0.0001$  to 0.012 (Fisher exact; Table 2). The agreement (all locations that were categorized as normal or abnormal in both eyes) ranged from 68% to 94% with the AC1 agreement coefficient ranging from 0.48 to 0.94 (Table 2). An 'overall agreement' of IT categorization of retinal locations from all 15 patients is shown in Table 3, and was significant with  $P < 0.0001$ , and 86% agreement (AC1 = 0.76).

Because the adolescents participating in this study did not have any diabetes-related complications, and have no other systemic diseases that should affect the eyes, one can expect high agreement in categorizing retinal locations due to a high prevalence of locations defined as normal in both eyes. The AC1 statistic partially eliminates a bias due to the high prevalence of locations categorized as normal, but not completely. As a final and conservative analysis, we eliminated the locations that were categorized as normal in both eyes, and looked only at retinal locations defined as abnormal in at least one eye. That allowed us to test whether the pattern of retinal locations defined as abnormal is indeed similar between the eyes. We evaluated the proportion of retinal locations defined as abnormal in both eyes (agreement between eyes) to the number of locations in which at least one eye was defined as abnormal, and tested whether it was significantly different from what is expected by chance. The 'overall agreement' was again significant with  $P < 0.0002$ .

The 'overall symmetry agreement' across subjects for mfERG AMP was also significant, with  $P < 0.0002$  (Fisher's exact). However, there was not sufficient statistical power to perform a more detailed analysis of symmetry due to the

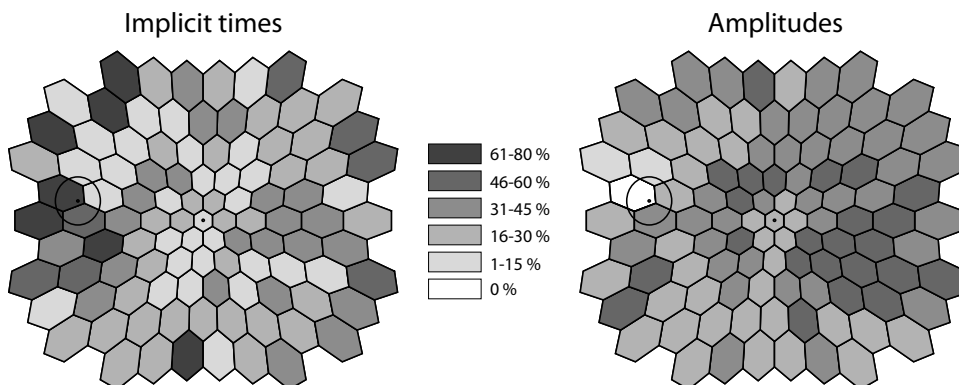


**FIGURE 2.** The percent of eyes (both eyes from each patient) with a Z-score  $\geq 2$  (for implicit times) or a Z-score  $\leq -2$  (for amplitudes), at each of the 103 hexagons is illustrated by the gray scale as indicated in the center. The percentage of eyes with abnormal mfERG implicit times (on left), and abnormal amplitudes (on right) at each of the 103 retinal locations. The gray scale plots are shown as left eyes in retinal view, with the circle representing the optic disc. The proportion of hexagons with abnormal implicit times is significantly higher in the nasal compared with temporal retina ( $P =$

0.015). The opposite is true with regard to hexagons with abnormal amplitudes ( $P = 0.0007$ ). The proportion of hexagons defined as abnormal was not different in the superior versus inferior retina for both implicit times or amplitudes ( $P = 0.9$  and 0.99, respectively).

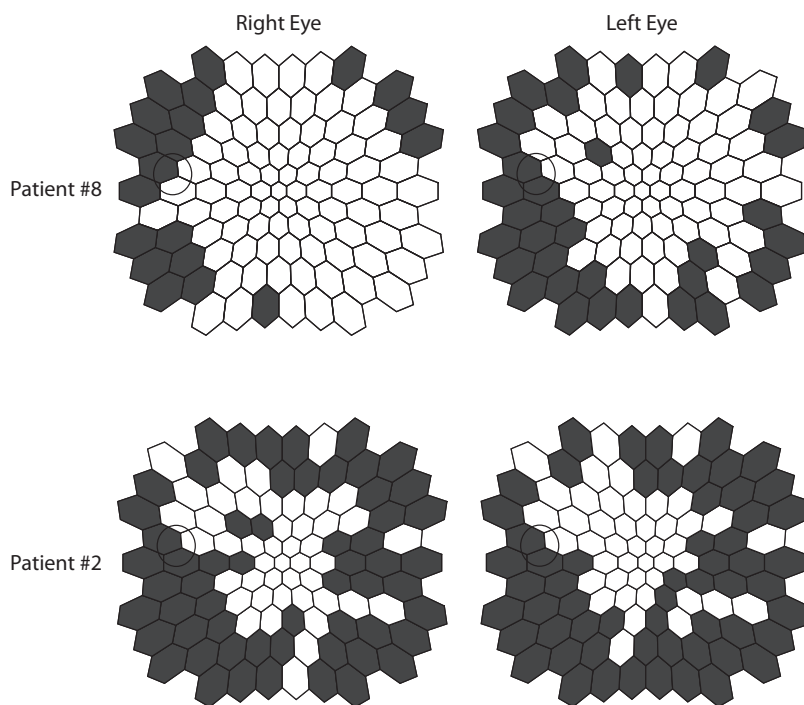


**FIGURE 3.** Examples of the similar distributions of hexagons defined as abnormal ( $Z$ -score  $\geq 2$  for implicit time) for two of the patients. Both eyes are plotted as left eyes for easier comparison, and abnormal locations are colored *black*.

relatively small sample size (only 5 patients had at least one eye defined as abnormal).

Two of the 15 patients analyzed here for IT symmetry have recently come for their 1-year follow up visit (patients 1 and 10). For both patients, the distributions of abnormal locations in the two eyes were highly symmetric in both visits (Table 4), even though there was mfERG IT worsening (i.e., a greater number of abnormal IT locations on visit 2 in one patient; HbA1c levels of 6.7% on visit 1 and 6.9% on visit 2), and mfERG IT improvement in the second patient (HbA1c levels of 11.2% on visit 1 and 9.6% on visit 2). Figure 4 shows the high interocular symmetry of abnormal IT locations for the two visits for one of these patients, despite the fact that the number of abnormalities greatly increased from visit 1 to visit 2.

**TABLE 2.** Percent of Agreement between Corresponding Locations with a Correction for Chance Agreement (AC1) and  $P$  Values, for Each of the Patients

Patient Number	Agreement (%)	AC1 Statistic	Fisher Exact $P$ Value
1	74	0.48	<0.0001
2	89	0.79	<0.0001
3	81	0.65	<0.0001
4	86	0.81	<0.0001
5	76	0.57	<0.0001
6	82	0.75	0.0004
7	93	0.91	<0.0001
8	81	0.68	<0.0001
9	87	0.84	0.002
10	94	0.93	<0.0001
11	93	0.92	0.004
12	68	0.50	0.002
13	94	0.94	N/A*
14	94	0.94	0.012
15	90	0.89	<0.0001

\* Two or more cells in the  $2 \times 2$  tables had a value of zero.

**DISCUSSION**

In this study, first order mfERG IT and AMP were evaluated in adolescents with type 1 diabetes and no retinopathy. Even though different subjects had different patterns of abnormal retinal function, individual subjects had very similar patterns in their two eyes. This observation strongly suggests that this novel finding of symmetry in the locations of abnormal IT between right and left eyes is not an artifact. Additional support for our symmetry findings are the two patients who had completed a 1-year follow-up appointment and showed symmetries in locations of retinal abnormalities in both visits, even in the case of increasing abnormalities.

Consistent with previous studies, we found delays in mfERG IT along with predominantly normal response AMP in patients with diabetes mellitus.<sup>7,8,23,24</sup> This phenomenon can be explained partly by the smaller variability in mfERG IT among eyes of healthy subjects compared with the greater variability of mfERG response amplitudes.<sup>7,23</sup> Another important contributing factor is that first order mfERG AMP appears to be less affected than mfERG IT at early stages of diabetic eye disease.<sup>7,25</sup>

The illustration in Figure 2 (left plot) shows that across patients many of the IT abnormalities are located around the optic nerve head. This is probably not an artifact related to the variable position of the optic nerve head across patients. There

**TABLE 3.** Agreement between Corresponding Locations in the Right versus Left Eyes across Patients (Overall Agreement from All 15 Patients)

	Right Eye	
	Abnormal	Normal
Left Eye		
Abnormal	307	143
Normal	81	1014

Agreement was 86%, AC1 = 0.76, with  $P < 0.0001$ .

**TABLE 4.** Agreement between Corresponding Locations in the Right versus Left Eyes for Two of the Patients in Their Initial and 1-Year Follow-Up Visits

Patient	Visit 1				Visit 2			
	Agreement	AC1 Statistic	Fisher Exact P Value	HbA1c	Agreement	AC1 Statistic	Fisher Exact P Value	HbA1c
1	74%	0.48	<0.0001	11.2%	76%	0.56	<0.0001	9.6%
10	94%	0.93	<0.0001	6.7%	83%	0.68	<0.0001	6.9%

is no reason to believe that the position of the optic nerve in patients with diabetes is different or more variable than in controls, and thus using Z-scores for analysis should eliminate the problem of having longer IT in the hexagons that correspond to the position of the optic nerve head. We cannot explain the nasal-temporal asymmetry in the distribution of locations with abnormal IT, however we haven't seen this bias previously in a group of adult patients with type 2 diabetes.<sup>26</sup>

As mentioned above, the mfERG AMPs were predominantly normal in the patients included in this study. This is not unexpected in young type 1 diabetes patients who are in otherwise good health and who have relatively short disease duration. However, the low frequency of AMP abnormalities is a potential limitation of the study because it limited our ability to examine in detail the potential interocular symmetry of the AMP abnormalities, due to insufficient statistical power. In addition, the nasal-temporal asymmetry in the distribution of AMP abnormalities as shown in Figure 2 could be related to the low number of patients with AMP abnormalities.

Interocular symmetry of locations with abnormal mfERG IT may be related to individual developmental predispositions at certain locations in both retinas that cause higher risk for developing the neural abnormalities reflected by mfERG delays. The source of these response delays may be microvascular (e.g., ischemic) in nature. Alteration in neural function measured as delayed mfERG IT in diabetic patients with good visual acuity was previously shown to be associated with reduced microcirculation and ischemia in the macular area as measured by fluorescein angiography.<sup>27</sup> Other studies also correlated

delays in mfERG IT with macular ischemia in patients with retinal vein occlusion.<sup>28,29</sup>

Clinically, diabetes-related retinal abnormalities were previously mainly associated with visible vasculature pathology. A major suspect in the pathogenesis of retinopathy is excess blood glucose concentration that creates oxidative stress, activation of protein kinase C (PKC), and advanced glycation end products.<sup>30-35</sup> These promote processes that eventually lead to the activation of mechanisms of vascular injury.<sup>35-37</sup>

Evidence for neural involvement in patients with diabetic retinopathy has been present from histopathologic studies over the past 40 years,<sup>35,38,39</sup> and a number of studies using electrophysiology, dark adaptation, and other psychophysical tests have shown reduction in neural function even before retinopathy was present.<sup>23,35,40-44</sup> Antonetti et al. (2006)<sup>35</sup> recently suggested a feed-forward process involving vascular as well as neuronal damage at early stages that leads to chronic inflammation in the retina, and eventually causes clinically recognized diabetic retinopathy.

The role neuropathy has in creating the clinical vascular signs of diabetic retinopathy was probably underestimated in the past because the neural retina is transparent, and cannot be visualized clinically by ophthalmoscopy or fluorescein angiography. As previously discussed, mfERG IT is a sensitive measure that can indicate neural damage even before clinical vascular abnormalities can be seen (and is also predictive of the vascular abnormalities), and thus can be used as a key tool in identifying diabetic retinal abnormalities at the earliest stages.

In conclusion, we found that, despite different patterns of functional abnormalities across patients, individual adolescents with type 1 diabetes and no retinopathy show symmetry in patterns of mfERG IT abnormalities between their right and left eyes. Interocular symmetry of locations with abnormal mfERG IT could be used in the design of clinical trials to test the efficacy of newly developed topical drugs. For example, treatment could be applied to only one eye while the fellow eye serves as a control. In the future, using the mfERG as a clinical tool for identifying retinal abnormalities and initiating treatment at early stages, before clinical retinopathy can be seen, may be beneficial for better prognosis. Treatment could be initiated in both eyes even if one eye has more abnormalities than the fellow eye, knowing that locations with abnormal mfERGs in one eye are likely to become abnormal in the fellow eye.

### Acknowledgments

The authors thank Brian Wolff, Glen Ozawa, and Kavita Dhamdhare for their help in testing patients, and Maria Cardenas and Guadalupe Barron for their help in data collection and analysis.

### References

- Caird FI, Pirie A, Ramsell TG. *Diabetes and the Eye*. Oxford, Edinburgh: Blackwell Scientific; 1969.

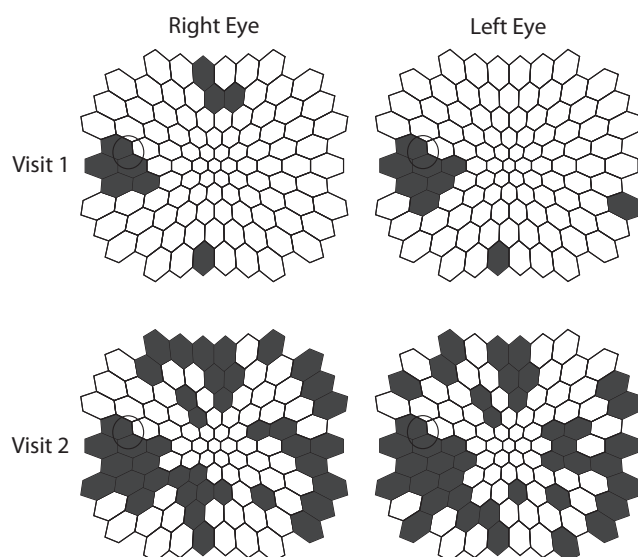


**FIGURE 4.** The retinal locations classified as abnormal for implicit time for patient 10 at the initial and 1-year follow-up appointments. At both appointments, there was significant symmetry of abnormal locations in the two eyes (colored in black).

2. Taylor E, Admitt PI, Jennings AMC. An analysis of diabetic retinopathy. *Quarterly Journal of Medicine*. 1973;New Series, XLII:305-315.
3. Javitt JC. Cost savings associated with detection and treatment of diabetic eye disease. *Pharmacoeconomics*. 1995;8(suppl 1):33-39.
4. Javitt JC, Aiello LP, Bassi LJ, Chiang YP, Canner JK. Detecting and treating retinopathy in patients with type 1 diabetes mellitus. Savings associated with improved implementation of current guidelines. American Academy of Ophthalmology. *Ophthalmology*. 1991;98:1565-1573, discussion 1574.
5. The Diabetes Control and Complications Trial Research Group. The effect of intensive treatment of diabetes on the development and progression of long-term complications in insulin-dependent diabetes mellitus. The Diabetes Control and Complications Trial Research Group. *N Engl J Med* 1993;329:977-986.
6. Early Treatment Diabetic Retinopathy Study Research Group. Early photocoagulation for diabetic retinopathy. ETDRS report number 9. Early Treatment Diabetic Retinopathy Study Research Group. *Ophthalmology* 1991;98:766-785.
7. Bearse MA Jr, Adams AJ, Han Y, et al. A multifocal electroretinogram model predicting the development of diabetic retinopathy. *Prog Retin Eye Res*. 2006;25:425-448.
8. Han Y, Bearse MA Jr, Schneck ME, Barez S, Jacobsen CH, Adams AJ. Multifocal electroretinogram delays predict sites of subsequent diabetic retinopathy. *Invest Ophthalmol Vis Sci*. 2004;45:948-954.
9. Han Y, Schneck ME, Bearse MA Jr, et al. Formulation and evaluation of a predictive model to identify the sites of future diabetic retinopathy. *Invest Ophthalmol Vis Sci*. 2004;45:4106-4112.
10. Harrison WW, Bearse MA, Ng JS, et al. Multifocal electroretinograms predict onset of diabetic retinopathy in adult patients with diabetes. *Invest Ophthalmol Vis Sci*. 2011;52:772-777.
11. Ng JS, Bearse MA Jr, Schneck ME, Barez S, Adams AJ. Local diabetic retinopathy prediction by multifocal ERG delays over 3 years. *Invest Ophthalmol Vis Sci*. 2008;49:1622-1628.
12. Bronson-Castain KW, Bearse MA Jr, Neuville J, et al. Adolescents with Type 2 diabetes: early indications of focal retinal neuropathy, retinal thinning, and venular dilation. *Retina*. 2009;29:618-626.
13. Bronson-Castain K, Bearse MAJ, Neuville J, et al. Early neural and vascular changes in the adolescent Type 1 and Type 2 diabetic retina. *Retina*. 2012;32:92-102.
14. Barondes M, Pauleikhoff D, Chisholm IC, Minassian D, Bird AC. Bilaterality of drusen. *Br J Ophthalmol*. 1990;74:180-182.
15. Bellmann C, Jorzik J, Spital G, Unnebrink K, Pauleikhoff D, Holz FG. Symmetry of bilateral lesions in geographic atrophy in patients with age-related macular degeneration. *Arch Ophthalmol*. 2002;120:579-584.
16. Hood D, Li J. A technique for measuring individual multifocal ERG records. In: Yager D, ed. *Trends in Optics and Photonics*. 1997;11:280-283.
17. Hood DC. Assessing retinal function with the multifocal technique. *Prog Retin Eye Res*. 2000;19:607-646.
18. Keating D, Parks S, Smith D, Evans A. The multifocal ERG: unmasked by selective cross-correlation. *Vision Res*. 2002;42:2959-2968.
19. Sutter EE. Imaging visual function with the multifocal m-sequence technique. *Vision Res*. 2001;41:1241-1255.
20. Cheng H, Laron M, Schiffman JS, Tang RA, Frishman LJ. The relationship between visual field and retinal nerve fiber layer measurements in patients with multiple sclerosis. *Invest Ophthalmol Vis Sci*. 2007;48:5798-5805.
21. Gwet KL. Computing inter-rater reliability and its variance in the presence of high agreement. *British Journal of Mathematical & Statistical Psychology*. 2008;61:29-48.
22. Gwet K. Inter-rater reliability: dependency on trait prevalence and marginal homogeneity. *Statistical Methods for Inter-Rater Reliability Assessment Series*. 2002;2:1-9.
23. Fortune B, Schneck ME, Adams AJ. Multifocal electroretinogram delays reveal local retinal dysfunction in early diabetic retinopathy. *Invest Ophthalmol Vis Sci*. 1999;40:2638-2651.
24. Greenstein VC, Holopigian K, Hood DC, Seiple W, Carr RE. The nature and extent of retinal dysfunction associated with diabetic macular edema. *Invest Ophthalmol Vis Sci*. 2000;41:3643-3654.
25. Palmowski AM, Sutter EE, Bearse MA Jr, Fung W. Mapping of retinal function in diabetic retinopathy using the multifocal electroretinogram. *Invest Ophthalmol Vis Sci*. 1997;38:2586-2596.
26. Han Y, Bearse MA Jr, Schneck ME, Barez S, Jacobsen C, Adams AJ. Towards optimal filtering of "standard" multifocal electroretinogram (mfERG) recordings: findings in normal and diabetic subjects. *Br J Ophthalmol*. 2004;88:543-550.
27. Tyrberg M, Ponjavic V, Lovestam-Adrian M. Multifocal electroretinogram (mfERG) in patients with diabetes mellitus and an enlarged foveal avascular zone (FAZ). *Doc Ophthalmol*. 2008;117:185-189.
28. Dolan FM, Parks S, Keating D, Dutton GN. Wide field multifocal and standard full field electroretinographic features of hemi retinal vein occlusion. *Doc Ophthalmol*. 2006;112:43-52.
29. Hvarfner C, Andreasson S, Larsson J. Multifocal electroretinography and fluorescein angiography in retinal vein occlusion. *Retina*. 2006;26:292-296.
30. Aiello LP. The potential role of PKC beta in diabetic retinopathy and macular edema. *Surv Ophthalmol*. 2002;47(suppl 2):S263-S269.
31. Barile GR, Pachydaki SI, Tari SR, et al. The RAGE axis in early diabetic retinopathy. *Invest Ophthalmol Vis Sci*. 2005;46:2916-2924.
32. Caldwell RB, Bartoli M, Behzadian MA, et al. Vascular endothelial growth factor and diabetic retinopathy: role of oxidative stress. *Curr Drug Targets*. 2005;6:511-524.
33. Hudson BI, Schmidt AM. RAGE: a novel target for drug intervention in diabetic vascular disease. *Pharm Res*. 2004;21:1079-1086.
34. Stitt AW. The role of advanced glycation in the pathogenesis of diabetic retinopathy. *Exp Mol Pathol*. 2003;75:95-108.
35. Antonetti DA, Barber AJ, Bronson SK, et al. Diabetic retinopathy: seeing beyond glucose-induced microvascular disease. *Diabetes*. 2006;55:2401-2411.
36. Antonetti DA, Lieth E, Barber AJ, Gardner TW. Molecular mechanisms of vascular permeability in diabetic retinopathy. *Semin Ophthalmol*. 1999;14:240-248.
37. Miyamoto K, Khosrof S, Bursell SE, et al. Prevention of leukostasis and vascular leakage in streptozotocin-induced diabetic retinopathy via intercellular adhesion molecule-1 inhibition. *Proc Natl Acad Sci U S A*. 1999;96:10836-10841.
38. Wolter JR. Diabetic retinopathy. *Am J Ophthalmol*. 1961;51:1123-1141.
39. Bloodworth JM Jr. Diabetic retinopathy. *Diabetes*. 1962;11:1-22.
40. Bearse MA Jr, Han Y, Schneck ME, Barez S, Jacobsen C, Adams AJ. Local multifocal oscillatory potential abnormalities in diabetes and early diabetic retinopathy. *Invest Ophthalmol Vis Sci*. 2004;45:3259-3265.
41. Bresnick GH. Diabetic retinopathy viewed as a neurosensory disorder. *Arch Ophthalmol*. 1986;104:989-990.
42. Ghirlanda G, Di Leo MA, Caputo S, Cercone S, Greco AV. From functional to microvascular abnormalities in early diabetic retinopathy. *Diabetes Metab Rev*. 1997;13:15-35.
43. Greenstein VC, Shapiro A, Zaidi Q, Hood DC. Psychophysical evidence for post-receptor sensitivity loss in diabetics. *Invest Ophthalmol Vis Sci*. 1992;33:2781-2790.
44. Parisi V, Uccioli L. Visual electrophysiological responses in persons with type 1 diabetes. *Diabetes Metab Res Rev*. 2001;17:12-18.